SEMARAK ILMU PUBLISHING

Journal of Advanced Research in Applied Mechanics

Journal homepage:
https://semarakilmu.com.my/journals/index.php/appl_mech/index
ISSN: 2289-7895

Optimization of Polyvinylidene Fluoride/Polyvinyl Alcohol Electrospun using Taguchi Method for Tissue Engineering Application

Mohd Syahir Anwar Hamzah[1,2], Nadirul Hasraf Mat Nayan[1,2,*], Norhana Jusoh[3]

[1] Oasis Integrated Group, Institute of Integrated Engineering, Universiti Tun Hussein Onn Malaysia, 86400 Parit Raja, Johor, Malaysia
[2] Department of Chemical Engineering Technology, Faculty of Engineering Technology, Universiti Tun Hussein Onn Malaysia, KM 1 Jalan Panchor, Pagoh Higher Education Hub, 84600 Panchor, Johor, Malaysia
[3] Department of Biomedical Engineering & Health Sciences, Faculty of Electrical Engineering, Universiti Teknologi Malaysia 81310 Skudai, Johor, Malaysia

ARTICLE INFO

Article history:
Received 31 July 2024
Received in revised form 2 September 2024
Accepted 9 September 2024
Available online 30 September 2024

Keywords:
Taguchi; Electrospinning; Tissue Engineering; Optimization; Nanofibers

ABSTRACT

Composite nanofibers for tissue engineering applications were prepared with polyvinylidene fluoride and polyvinyl alcohol via a horizontal electrospinning process. The effect of the processing parameters (polymer concentration, voltage, feed rate and tip-to-collector distance) on the fibre diameter was studied using L9 orthogonal arrays of the Taguchi Method, S/N ratio, and ANOVA to produce uniform and finest fibre. The optimum parameters were at 90 wt% PVDF ratios for polymer concentration, applied voltage at 10 kV, feed rate at 0.5 mL/h and tip-to-collector distance at 15 cm. The PVDF/PVA electrospun compromises 171.60 nm nanofiber diameter with homogenous morphology and no bead formed. MTT and live/dead kit assay analysis toward human (HSF) cells confirmed the potential of the PVDF/PVA electrospun to be used as an alternative tissue template to allow new cell or tissue formation in the future.

1. Introduction

The similarity between electrospun fibres and native tissues has led to the recognition of electrospinning as one of the most effective procedures. Nanofibrous scaffolds have been created during the past few decades for a dizzying array of biological uses, including tissue regeneration and the transport of medicinal agents [1]. Electrospun scaffolds have several advantages over other fabrication methods due to their functional complexity. However, more work must be done before they can be used in vivo to their full potential. Electrospinning nanofibers have several inherent advantages, including the capacity to precisely control material and mechanical properties, the production of substrates with high surface area-to-volume ratios, and a propensity for cellular in-growth brought on by interconnectivity within the pores [2-4]. Additionally, the electrospinning method enables the creation of scaffolds with topographies on the micro to nanoscale that mimic

* *Corresponding author.*
E-mail address: nadirul@uthm.edu.my

https://doi.org/10.37934/aram.125.1.8192

the extracellular matrix (ECM) in nature. In order to match the rate of regeneration of the damaged tissue and ensure the development of non-toxic breakdown products that the body can quickly eliminate, electrospun needs to be tailored, a concept that researchers are still exploring.

Electrospinning starts when an electron from the applied electric charge is transferred via a metallic needle to the polymer solution. The polymer solution becomes unstable, which causes the polymer droplet to acquire a charge [1,5]. The force produced by the simultaneous reciprocal repulsion of charges eventually overcomes surface tension and forces the polymer solution to flow in the direction of the electric field [6]. An increase in the electric field deforms spherical droplets. At that point, Taylor cones, conical polymer droplets positioned atop metallic collectors kept at an ideal distance, start forming ultrafine nanofibers [7,8]. The smooth and consistent nanofiber architectures can be influenced by the solution parameters (solvent, polymer concentration viscosity and solution conductivity), process setup (applied voltage, distance between the needle and collector, flow rate) and external factors, including temperature and humidity [2-4,9-11]. Therefore, choosing the electrospinning conditions would be crucial to creating the required morphology with uniform, bead-free and evenly distributed fibres.

Controlling the fibre diameter, for instance, continues to be a methodological barrier. In this study, the spinning parameter of the electrospinning process was optimized using Taguchi Method and analyzed using Minitab Software to produce polyvinylidene fluoride / polyvinyl alcohol nanofibers. The process parameters such as polymer concentration (PVDF wt% ratio), voltage, feed rate, and tip-to-collector distance factors were studied with diameter nanofiber as output. The orthogonal arrays developed by Dr. Genichi Taguchi were used in designing the statistical model due to their capability to make selections based on the number of parameters in the experiment and the number of levels. Besides, a minimum of trials could also be used to identify the factors that affect product quality by evaluating the factors separately or jointly [12-15].

This study will use a rare semi-crystalline conductive polyvinylidene fluoride polymer (PVDF) as a main resin in producing nanofiber membrane wound dressing. An earlier investigation into the electrospinning of PVDF revealed the polar β-phase crystal's dominant orientation crystalline structure along a fibre axis, which results in high electric conductivity behaviours that make it appropriate for tissue engineering [16]. Several researchers reported on the incorporation of PVDF with other materials such as cellulose acetate, polyurethane (PU), enrofloxacin (Enro), hyaluronic acid (HA), and polyvinyl alcohol (PVA) to increase its water absorption ability without losing its mechanical integrity for enhancing specific cell recognition sites [17-19]. None of them has focused on optimizing the spinning parameters to predict fibre diameter, especially involving polymer modification.

Our current manuscript builds on the preliminary findings we published in Hamzah *et al.,* (2021) [20]. In the previous study, we identified key factors influencing the production of PVDF/PVA electrospun. This present work aims to delve deeper into these parameter factors, examining their implications in greater detail and expanding the scope to optimize the electrospinning process. To identify the ideal process variable that impacts the diameter of the electrospun fibre, this work intends to investigate the impact of electrospinning parameters on PVDF/PVA nanofiber shape. The optimization process will help yield the finest fibres that meet the tissue engineering requirements which were confirmed by in-vitro human skin cell culture analysis.

2. Methodology

2.1 Preparation of Electrospinning Solution

The polyvinylidene fluoride (PVDF, MW≈534000 g/mol) was dissolved in dimethyl sulfoxide (DMSO) solvent with polyvinyl alcohol (PVA, MW≥89000 g/mol) forming 0.15 % (w/v). Different PVDF-to-PVA ratios at 85/15, 90/10, and 95/5 were dissolved in the solvent and stirred at room temperature for two hours, forming homogenous electrospinning solutions [20]. The suspension solution was drawn into a 5 mL syringe with a 23-gauge needle size and placed at a horizontally set up electrospinning apparatus (Figure 1). The electrospinning process was done in 1 hour with a range of voltage 10 – 15 kV, flow rate at 0.5 – 1.5 mL/h, and 15 – 19 cm tip-to-collector distance at ambient conditions.

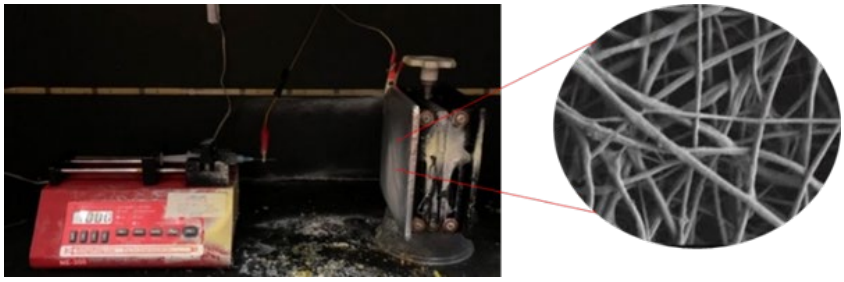

Fig. 1. A horizontal electrospinning setup was used in the experiment

2.2 Taguchi Design

In this paper, the major variables and interactions can be explored using Taguchi's technique with the fewest possible trials. Four factors (polymer concentration which is PVDF wt% ratio, voltage, flow rate, and tip-to-collector distance) were used in the L9 orthogonal array at 3 different levels, as shown in Table 1. Minitab 17 software was used to construct an orthogonal array, obtaining only nine experiments would be conducted instead of 81 experiments as illustrated in Table 2 [14].

Table 1
Selected factors and their levels used in Taguchi design

	(A) PVDF wt% ratio	(B) Voltage, kV	(C) Flow rate, mL/h	(D) Tip-to-collector distance, cm
Level 1	85	10.0	0.5	15
Level 2	90	12.5	1.0	17
Level 3	95	15.0	1.5	19

*Setting conditions are Level 1: Low, Level 2: Intermediate, Level 3: High

Table 2
Experimental trials according to L9 orthogonal array

Sample No.	Designation	(A)	(B)	(C)	(D)
S1	$A_1B_1C_1D_1$	85	10.0	0.5	15
S2	$A_1B_2C_2D_2$	85	12.5	1.0	17
S3	$A_1B_3C_3D_3$	85	15.0	1.5	19
S4	$A_2B_1C_2D_3$	90	10.0	1.0	19
S5	$A_2B_2C_3D_1$	90	12.5	1.5	15
S6	$A_2B_3C_1D_2$	90	15.0	0.5	17
S7	$A_3B_1C_3D_2$	95	10.0	1.5	17
S8	$A_3B_2C_1D_3$	95	12.5	0.5	19
S9	$A_3B_3C_2D_1$	95	15.0	1.0	15

(A) – PVDF wt% ratio; (B) – Voltage (kV); (C) – Feed rate (mL/h); (D) – Tip-to-collector distance (cm)

Before getting the optimal circumstances for the best quality before being submitted to In-vitro cytotoxicity investigation using HDF cells, the DOE step will transform data from Table 2 to signal-to-noise ratio comparing to adjustable fibre diameter factors to explore the sensitivity of each factor [14,15,21]. In the Taguchi method, the Signal-to-Noise (S/N) ratio plays a crucial role in optimizing the performance of a system or process [13,21]. The S/N ratio is a metric used to quantify the quality characteristics of a product or process, and it is used to assess the effect of various factors on the output. The "smaller-the-better" approach was used to get the S/N ratio values using the relation shown in Eq. (1):

$$S/_N = -10\log(\frac{1}{n}\sum_{i=i}^{n} y_i^2) \quad (1)$$

where n is the number of observations in each experiment, and y_i is the measured response data.

The analysis of variance (ANOVA) was used to measure and categorize the predominant effect of the different variables in the form of the degree of freedom (DOF), the adjusted sum of squares (Adj SS), adjusted mean squares (Adj MS), and per cent contribution values. The percentage contribution can be calculated by using Eq. (2):

$$P_i = \frac{V_i}{V_T} x\ 100 \quad (2)$$

where V*i* is the variance at factors and V_T is total variance.

The confirmation experiment was carried out to confirm the reliability and reproducibility of the data specified in Eq. (1) to confirm the confidence in the optimal parameter from Taguchi analysis. To compare both data sets (experiment and estimated), the estimated S/N ratio using the optimum levels of the production parameters can be calculated as Eq. (3):

$$S/_{N_{estimated}} = S/_{N_M} + \sum_{i=1}^{n}(S/_{N_i} - S/_{N_M}) \quad (3)$$

S/N_M is the mean of the S/N ratios for each parameter level where S/N_i is the S/N ratio for the at *i* level. Then, the "estimated average diameter" can be calculated by using the relation Eq. (4):

$$S/_{N_{estimated}} = -10\log\ (d^2_{estimated}) \quad (4)$$

After substituting the optimum parameter levels into the above equations, the estimated S/N ratio and the estimated average fibre diameter were determined. The confidence level or accuracy of the Taguchi method in this could be quantified by using the following relation Eq. (5):

$$Accuracy = 100 - \left(\frac{Experimental\ Value - Estimated\ Value}{Estimated\ Value} x100\right) \quad (5)$$

2.3 Morphological Characterization of Electrospun Fiber

For morphological analysis of PVDF/PVA nanofiber, the JEOL Field Emission Scanning Electron Microscope (FESEM) model JSM-7800F was employed. Gold was sputtered onto the nanofiber for 30 seconds at a magnification of 100 to 10,000 x at 18 Ma. Using the software ImageJ to examine at least 100 distinct fibers, the diameter of the nanofiber was determined [20].

2.4 In-vitro Cytotoxicity Analysis

Human Skin Fibroblast (HSF 1184) cells were cultured in T-flasks containing DMEM medium supplemented with fetal bovine serum, penicillin-streptomycin, and pyruvate where all mediums are from Thermo Fisher Scientific. The cells were incubated at 37 ^{o}C with 5% CO_2 before undergoing cytotoxicity analysis. The sample will be seeded with HSF cell suspension at $1x10^4$ cells/mL for 24 hours. MTT assay was performed by quantifying the purple formazan crystals absorbance which represents the number of surviving cells after 24 hours by measuring the absorbance at 570 nm using a microplate reader [22]. The cells will be treated with Trixton-X for positive control and normal culturing for negative control. The samples were stained with Live/Dead kit assay to assess the cell viability and the image was captured using an inverted fluorescence microscope.

3. Results

3.1 Optimum Combination in Optimizing the PVDF/PVA Electrospun

In the optimization of electrospinning, the diameter characteristic of the fibres produced is an important parameter to consider. The diameter of the electrospun fibres significantly impacts their properties and performance in various applications. The FE-SEM micrographs of the composite fibre morphology are illustrated in Figure 2 and the corresponding average fibre diameters are tabulated in Table 3. Generally, fibres with smaller diameters exhibit higher mechanical strength due to reduced defects and higher orientation of polymer chains. Other than that, electrospun fibres have an extremely high surface area-to-volume ratio with greater porosity and interconnectedness of pores due to their small diameter, which is advantageous for applications such as tissue engineering and drug delivery [9,20,23]. As electrospinning relies on the electrostatic forces to form fibres, the diameter will influence the conductivity and charge distribution that contribute to the even release rate of encapsulated drugs or active agents in the materials [24]. By fine-tuning the electrospinning process using Taguchi in this study, the process parameter was optimized to find the best fibre diameter to improve performance and functionality.

Table 3
Diameter of PVDF/PVA electrospun and signal-to-noise (S/N) ratios based on "smaller is better."

Sample No.	Designation	Diameter nanofiber	S/N Ratio
S1	$A_1B_1C_1D_1$	172.00 (±37)	-44.7106
S2	$A_1B_2C_2D_2$	175.67 (±72)	-44.8940
S3	$A_1B_3C_3D_3$	175.27 (±64)	-44.8742
S4	$A_2B_1C_2D_3$	172.67 (±31)	-44.7443
S5	$A_2B_2C_3D_1$	176.00 (±50)	-44.9103
S6	$A_2B_3C_1D_2$	171.65 (±29)	-44.6929
S7	$A_3B_1C_3D_2$	175.32 (±36)	-44.8766
S8	$A_3B_2C_1D_3$	174.33 (±42)	-44.8274
S9	$A_3B_3C_2D_1$	173.30 (±68)	-44.7760

(A) – PVDF wt% ratio; (B) – Voltage (kV); (C) – Feed rate (mL/h); (D) – Tip-to-collector distance (cm)

The fibre diameter results from ImageJ analysis and were introduced into Minitab 17 software to gain the S/N ratio and p-value—generally, the higher the S/N ratio, the smaller the nanofiber diameters. Because a stand-alone mesh collector has minimal control over fiber alignment, random fiber distribution is visible in most electrospun mat samples. As observed, the PVDF/PVA electrospun have randomly oriented nanofibers with smooth surfaces and are homogenously distributed, where

some were detected with minor beads presence as typical defects on electrospun samples noticed in Figure 2 (b, h and i). However, after a quick look at the FESEM micrographs, the sample in Figure 2 (a, f and g) has a smaller diameter than other runs.

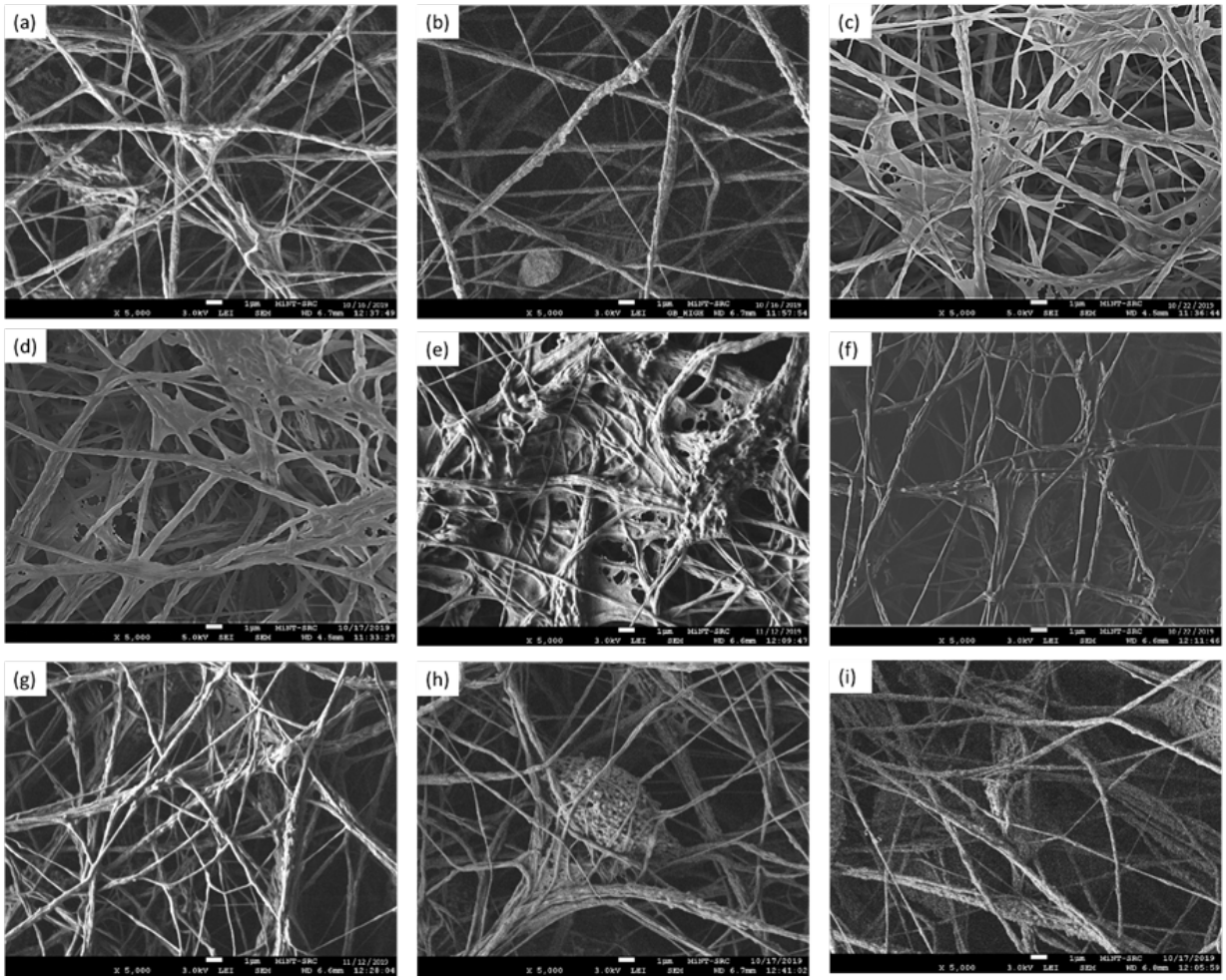

Fig. 2. FESEM images of PVDF/PVA fibres used in the design of experiments study: (a) S1; (b) S2; (c) S3; (d) S4; (e) S5; (f) S6; (g) S7; (h) S8 and (i) S9 at 5000x magnification

The main effects for S/N ratios were plotted using Minitab 17 software, as indicated in Table 3 and Figure 3. From the table, the most significant S/N ratio corresponds to the most minor electrospun fibre diameter obtained in the experiment. The nanofibers obtained in Run S6 have a minor diameter, followed by Run S1 and S4, as illustrated with the FESEM images of the smooth and almost bead-free electrospun fibre morphology that could be obtained from the designated runs. However, the S/N ratios plot suggested that combining the highest S/N ratio for each parameter may produce the optimum output. The ideal setting of fiber diameter-related parameters was $A_2B_1C_1D_1$, as indicated in Figure 3, which means that the experimental conditions should be set to have a PVDF concentration at 90 wt% (A), the voltage at 10.0 kV (B), feed rate at 0.5 mL/h (C) and 15 cm distance from the tip of needle gauge to a collector (D).

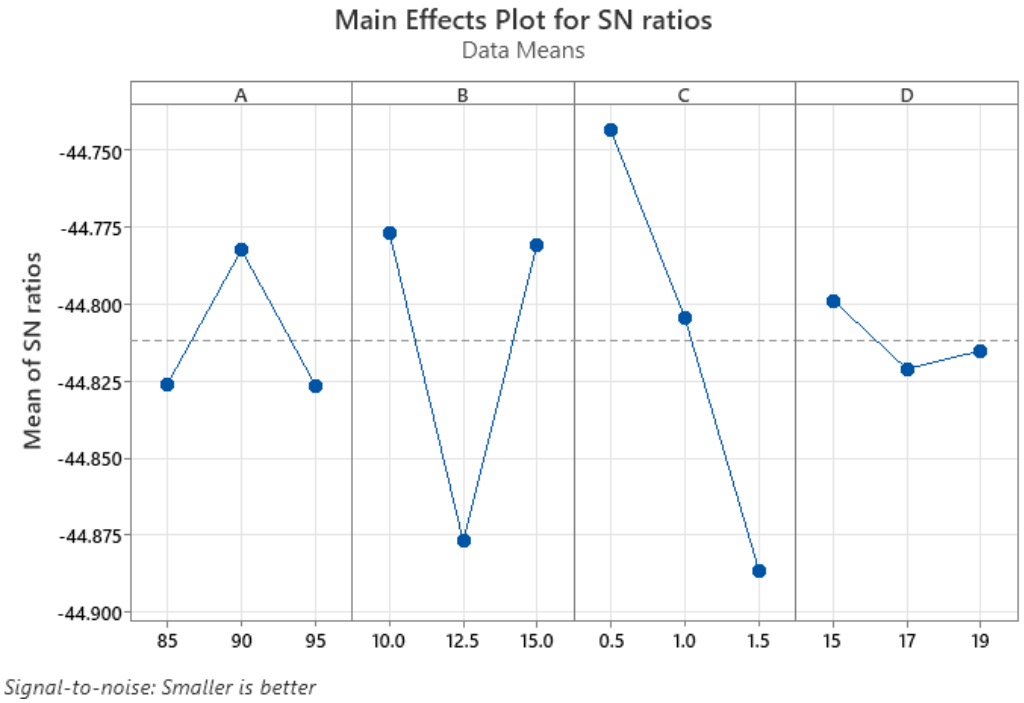

Fig. 3. Main effects plot for the S/N ratios of the experimental run

In Table 4, the delta value is the difference between the maximum and minimum S/N ratios. At the same time, the rank represents the importance of the processing parameters determined by ranking the delta values from the largest to the smallest. The degree of influence of the factors on the fibre diameter increased in the order of feed rate > voltage > PVDF wt% (polymer concentration) > tip-to-collector distance. The ANOVA was applied to the data set to determine each process parameter's contribution to confirm the different factors' specific influence on the quality characteristic. Table 5 tabulates the degree of freedom (DOF), the adjusted sum of squares (Adj SS), adjusted mean squares (Adj MS), and per cent contribution values. The results showed that the contributions of the individual factors to the fibre diameter were 5.58 % for the PVDF wt%, 34.14 % for voltage, 55.87 % for the feed rate, and 2.01 % for tip-to-collector distance. Besides, the feed rate has the highest F-value (the lowest p-value) among other parameters, which shows that it is the most critical parameter. Therefore, it can be concluded that the "importance ranking" data of the Taguchi S/N response approach directly coincides with the "per cent contribution" data of the ANOVA approach. The indication of feed rate, also known as flow rate, as the main factor contributing to diameter fibre characteristic is aligned with other studies.

Table 4
S/N ratio response table including delta and rank data

Level	A	B	C	D
1	-44.83	-44.78	-44.74	-44.80
2	-44.78	-44.88	-44.80	-44.82
3	-44.83	-44.78	-44.89	-44.82
Delta	0.04	0.10	0.14	0.002
Rank	3	2	1	4

Table 5
Analysis of variance for signal-to-noise ratios of electrospun PVDF/PVA fibre diameter

Source	DF	Seq SS	Adj MS	F	P	PCR (%)
A	2	0.003866	0.001933	0.22	0.806	5.58%
B	2	0.019280	0.009640	1.62	0.273	34.14%
C	2	0.031061	0.015530	3.90	0.082	55.87%
D	1	0.000796	0.000398	0.04	0.957	2.40%
Residual Error	2	0.002980				2.01%
Total	9	0.055003				100

DF: degree of freedom; SS: sum of squares; MS: mean of squares; PCR: percentage contribution ratio

The feed rate affects several parameters during the electrospinning process, including the nanofibers' jet initiation, stretching, and solidification. Generally, a higher feed rate tends to result in larger nanofibers, while a lower feed rate can lead to smaller nanofibers. This relationship arises due to the dynamics of the electrospinning process. The increased flow rate of the polymer solution or melt at higher feed rates can lead to thicker and faster jet initiation from the spinneret [25,26]. The higher jet velocity and increased stretching forces during flight can form thicker nanofibers upon solidification. Conversely, reducing the feed rate decreases the jet initiation speed and stretching forces, promoting the formation of thinner nanofibers [23,26].

3.2 Confirmation Eexperiment for the PVDF/PVA Nanofibers

The confirmation experiment was set up using $A_2B_1C_1D_1$ parameters combination of PVDF concentration at 90 wt% (A), the voltage at 10.0 kV (B), feed rate at 0.5 mL/h (C), and tip-to-collector distance at 15 cm (D). Figure 4 shows the morphology image of the PVDF/PVA electrospun after the confirmation experiment, along with their diameter frequency and diameter distribution histograms. The average diameter of the experimental PVDF/PVA electrospun fibres was determined as 171.60 (±21) nm, and the S/N ratio as -44.6802 as determined in Table 6. The estimated S/N ratio and the average fibre diameter were slightly lower than the experimental value. Overall, the confidence level or accuracy of the Taguchi method in this study was as large as 99 %.

The diameter of nanofibers suitable for tissue healing can vary depending on the specific application and desired outcomes. However, generally, nanofibers with diameters in the range of tens to hundreds of nanometers have shown promise for tissue healing. For example, in nerve tissue engineering, nanofibers with smaller diameters, 100-500 nm or even below 100 nm, are often used [27,28]. The smaller diameter nanofibers provide physical guidance and cues for the directional growth of axons in nerve regeneration. They can facilitate the formation of aligned neural networks and enhance the regrowth of damaged nerve fibres [19,27]. It is also similar to the native extracellular matrix (ECM) fibres found in the skin, which help mimic the natural tissue environment and promote cell attachment, migration, and regeneration.

Table 6
Result of the confirmation experiment for the diameter of PVDF/PVA nanofibers

	Condition	Nanofiber diameter nm	S/N ratio
Estimate	$A_2B_1C_1D_1$	171.13	-44.6668
Experimental	$A_2B_1C_1D_1$	171.60	-44.6802

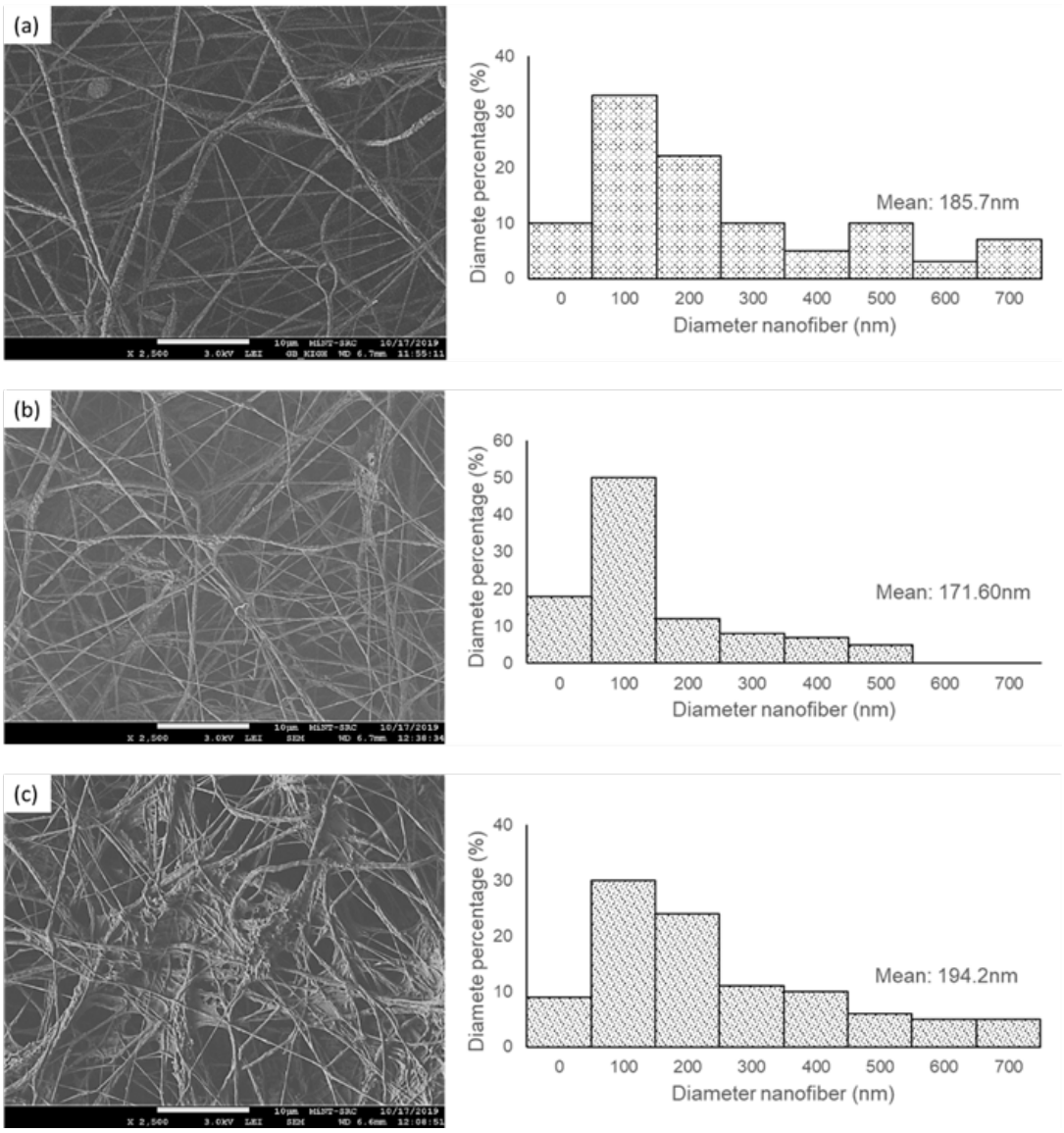

Fig. 4. The FESEM micrographic images and diameter nanofiber of (a) neat PVDF (b) optimum PVDF/PVAa (0.5 mL/h) and (c) PVDF/PVAb at 80 wt% PVDF, 15kV, 1.5 mL/h and 19 cm tip-to-collector distance

3.3 In-Vitro Cytotoxicity Analysis

In-vitro cell culture exposed to the negative control, positive control and PVDF/PVA sample under optimal conditions, the viability was 95.80±5.1%, 26.28±4.2% and 87.41±4.6% at 24 hours of continued growth in the culture as shown in Figure 5(a). The optimized electrospun has nontoxic potential to be used in tissue engineering applications where the cell viability increases to >50% compared to the positive control, which has lower cell viability. The micrographic image of cell viability confirmed the results in Figures 5(b). As a result of its hierarchical structure of linked pores, which created a favorable environment for cell meiosis, this suggested that the ideal fiber architecture of PVDF/PVA electrospun might facilitate the attachment and proliferation of the HSF cells. This corroborates another suggestion that suggests the range of nanofibers should be between 20 and 400 nm to support the infiltration of human cells with higher porosities to favour cell infiltration [29-31].

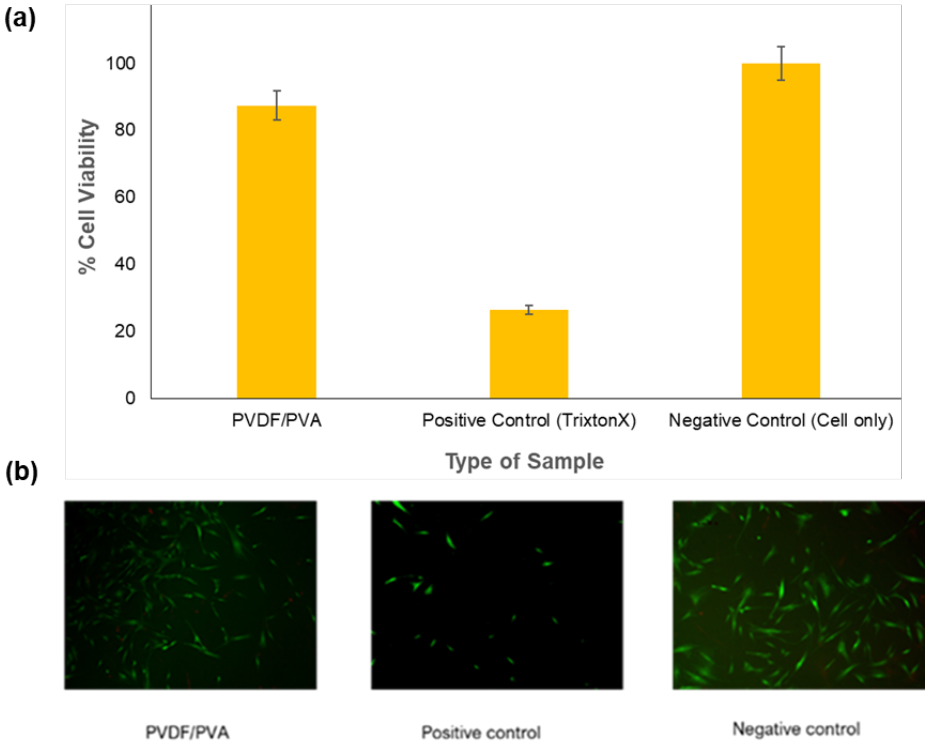

Fig. 5. (a) Percentage of cell viability; (b) microscopic image of cells and (c) fluorescent image of cells from different cultured condition

4. Conclusions

PVDF/PVA fibres were electrospinning based on 4 factors of an L9 orthogonal array with S/N ratios and ANOVA in the Taguchi Method. The PVDF wt% (polymer concentration), voltage, feed rate and tip-to-collector distance at 3 different levels were studied to investigate the optimal factor levels for a thinner fibre diameter during electrospinning. The feed rate was found to be the most influential factor in the diameter of PVDF/PVA fibres. The smaller diameter was produced at a low feed rate during the spinning process. The combination of the $A_2B_1C_1D_1$ parameters was the optimum process condition and was subjected to further characterization studies. The optimum electrospun fibre was evaluated with the neat PVDF and PVDF/PVA with larger nanofiber diameter by increasing the feed rate parameter to 1.5 mL/h to differentiate the properties of the samples. The optimum PVDF/PVA electrospun was found to have good biocompatibility properties with low toxic potential towards human cells, as indicated by MTT and live/dead kit assay. Therefore, the Taguchi Method was successfully applied to optimize the electrospinning conditions for PVDF/PVA nanofibers with minimal trial, producing a good, desired outcome for tissue engineering application.

Acknowledgement

This research was funded by a Fundamental Research Grant Scheme (FRGS) FRGS/1/2022/TK09/UTHM/03/7 from Ministry of Higher Education of Malaysia and Universiti Tun Hussein Onn Malaysia through Geran Penyelidikan Pascasiswazah (GPPS - H458).

References

[1] Petty, Anthony J., Rebecca L. Keate, Bin Jiang, Guillermo A. Ameer, and Jonathan Rivnay. "Conducting polymers for tissue regeneration in vivo." *Chemistry of Materials* 32, no. 10 (2020): 4095-4115. https://doi.org/10.1021/acs.chemmater.0c00767

[2] Jun, Indong, Hyung-Seop Han, James R. Edwards, and Hojeong Jeon. "Electrospun fibrous scaffolds for tissue engineering: Viewpoints on architecture and fabrication." *International journal of molecular sciences* 19, no. 3 (2018): 745. https://doi.org/10.3390/ijms19030745
[3] Chen, Hua-Wei, and Min-Feng Lin. "Characterization, biocompatibility, and optimization of electrospun SF/PCL/CS composite nanofibers." Polymers 12, no. 7 (2020): 1439. https://doi.org/10.3390/polym12071439
[4] Feng, Yanping, Zhang Jupei, Zhihong Dong, and Lu Tang. "Characterization, biocompatibility, and optimization of electrospun SF/PCL composite nanofiber films." Reviews on Advanced Materials Science 62, no. 1 (2023): 20220333. https://doi.org/10.1515/rams-2022-0333
[5] Ahmadian, Amirhossein, Abbas Shafiee, Nojan Aliahmad, and Mangilal Agarwal. "Overview of nano-fiber mats fabrication via electrospinning and morphology analysis." Textiles 1, no. 2 (2021): 206-226. https://doi.org/10.3390/textiles1020010
[6] Haider, Adnan, Sajjad Haider, and Inn-Kyu Kang. "A comprehensive review summarizing the effect of electrospinning parameters and potential applications of nanofibers in biomedical and biotechnology." *Arabian Journal of Chemistry* 11, no. 8 (2018): 1165-1188. https://doi.org/10.1016/j.arabjc.2015.11.015
[7] Ramakrishna, Seeram. *An introduction to electrospinning and nanofibers*. World scientific, 2005. https://doi.org/10.1142/9789812567611_0003
[8] Smith, James A., and Elisa Mele. "Electrospinning and additive manufacturing: adding three-dimensionality to electrospun scaffolds for tissue engineering." Frontiers in bioengineering and biotechnology 9 (2021): 674738. https://doi.org/10.3389/fbioe.2021.674738
[9] Chinnappan, Balaji Ayyanar, Marimuthu Krishnaswamy, Huaizhong Xu, and Md Enamul Hoque. "Electrospinning of biomedical nanofibers/nanomembranes: effects of process parameters." Polymers 14, no. 18 (2022): 3719. https://doi.org/10.3390/polym14183719
[10] Horuz, Tuğba İnanç, and K. Bülent Belibağlı. "Production of electrospun gelatin nanofibers: an optimization study by using Taguchi's methodology." *Materials Research Express* 4, no. 1 (2017): 015023. https://doi.org/10.1088/2053-1591/aa57ea
[11] Asiri, Amnah, Rania Hussien Al-Ashwal, Mohd Helmi Sani, and Syafiqah Saidin. "Effects of electrospinning voltage and flow rate on morphology of poly-vinyl alcohol nanofibers." In *Journal of Physics: Conference Series*, vol. 1372, no. 1, p. 012035. IOP Publishing, 2019. https://doi.org/10.1088/1742-6596/1372/1/012035
[12] Davis, Rahul, and Pretesh John. "Application of Taguchi-based design of experiments for industrial chemical processes." *Statistical approaches with emphasis on design of experiments applied to chemical processes* 137 (2018). https://doi.org/10.5772/intechopen.69501
[13] Rao, Ravella Sreenivas, C. Ganesh Kumar, R. Shetty Prakasham, and Phil J. Hobbs. "The Taguchi methodology as a statistical tool for biotechnological applications: a critical appraisal." *Biotechnology Journal: Healthcare Nutrition Technology* 3, no. 4 (2008): 510-523. https://doi.org/10.1002/biot.200700201
[14] Abbas, Jamal A., Ibtisam A. Said, Manaf A. Mohamed, Suhad A. Yasin, Zeravan A. Ali, and Idrees H. Ahmed. "Electrospinning of polyethylene terephthalate (PET) nanofibers: Optimization study using taguchi design of experiment." In *IOP conference series: materials science and engineering*, vol. 454, p. 012130. IOP Publishing, 2018. https://doi.org/10.1088/1757-899X/454/1/012130
[15] Wu, Chang-Mou, Ching-Hsiang Hsu, Ching-Iuan Su, Chun-Liang Liu, and Jiunn-Yih Lee. "Optimizing parameters for continuous electrospinning of polyacrylonitrile nanofibrous yarn using the Taguchi method." *Journal of Industrial Textiles* 48, no. 3 (2018): 559-579. https://doi.org/10.1177/1528083717740741
[16] Correia, Daniela M., Clarisse Ribeiro, Vitor Sencadas, Gabriela Botelho, S. A. C. Carabineiro, JL Gomes Ribelles, and Senentxu Lanceros-Méndez. "Influence of oxygen plasma treatment parameters on poly (vinylidene fluoride) electrospun fiber mats wettability." *Progress in Organic Coatings* 85 (2015): 151-158. https://doi.org/10.1016/j.porgcoat.2015.03.019
[17] Moradi, Rasoul, Javad Karimi-Sabet, Mojtaba Shariaty-Niassar, and Mohammad A. Koochaki. "Preparation and characterization of polyvinylidene fluoride/graphene superhydrophobic fibrous films." *Polymers* 7, no. 8 (2015): 1444-1463. https://doi.org/10.3390/polym7081444
[18] Kim, Young Kwang, Sung-Ho Hwang, Hye-Jin Seo, Soon Moon Jeong, and Sang Kyoo Lim. "Effects of biomimetic cross-sectional morphology on the piezoelectric properties of BaTiO3 nanorods-contained PVDF fibers." *Nano Energy* 97 (2022): 107216. https://doi.org/10.1016/j.nanoen.2022.107216
[19] Hamzah, Mohd Syahir Anwar, Nurul Amira Ab Razak, Celine Ng, Jumadi Abdul Sukor, Saiful Izwan Abd Razak, and Nadirul Hasraf Mat Nayan. "A Brief Review on Prospective of Polyvinylidene Fluoride as a Tissue Engineered Scaffold Material." *Journal of Advanced Industrial Technology and Application* 1, no. 2 (2020): 12-22. https://doi.org/10.30880/jaita.0000.00.00.000
[20] Hamzah, Mohd Syahir Anwar, Nurul Amira Ab Razak, Celine Ng, Akmal Hafiszi Abdul Azize, Jumadi Abdul Sukor, Soon Chin Fhong, Mohd Safiee Idris, and Nadirul Hasraf Mat Nayan. "Preparation of the electrospun polyvinylidene

fluoride/polyvinyl alcohol scaffold as a potential tissue replacement." IIUM Engineering Journal 22, no. 1 (2021): 245-258. https://doi.org/10.31436/iiumej.v22i1.1548

[21] Meyva-Zeybek, Yelda, and Cevdet Kaynak. "Electrospinning of PLA and PLA/POSS nanofibers: Use of Taguchi optimization for process parameters." Journal of Applied Polymer Science 138, no. 3 (2021): 49685. https://doi.org/10.1002/app.49685

[22] Feoktistova, Maria, Peter Geserick, and Martin Leverkus. "Crystal violet assay for determining viability of cultured cells." *Cold Spring Harb Protoc* 2016, no. 4 (2016): 343-6. https://doi.org/10.1101/pdb.prot087379

[23] Wang, Xiao-Xiong, Gui-Feng Yu, Jun Zhang, Miao Yu, Seeram Ramakrishna, and Yun-Ze Long. "Conductive polymer ultrafine fibers via electrospinning: Preparation, physical properties and applications." *Progress in Materials Science* 115 (2021): 100704. https://doi.org/10.1016/j.pmatsci.2020.100704

[24] Sill, Travis J., and Horst A. Von Recum. "Electrospinning: applications in drug delivery and tissue engineering." *Biomaterials* 29, no. 13 (2008): 1989-2006. https://doi.org/10.1016/j.biomaterials.2008.01.011

[25] Valizadeh, A. and Mussa Farkhani, S., 2014. Electrospinning and electrospun nanofibres. *IET nanobiotechnology*, *8*(2), pp.83-92. https://doi.org/10.1049/iet-nbt.2012.0040

[26] Henriques, C., R. Vidinha, D. Botequim, J. P. Borges, and J. A. M. C. Silva. "A systematic study of solution and processing parameters on nanofiber morphology using a new electrospinning apparatus." *Journal of nanoscience and nanotechnology* 9, no. 6 (2009): 3535-3545. https://doi.org/10.1166/jnn.2009.ns27

[27] Sill, Travis J., and Horst A. Von Recum. "Electrospinning: applications in drug delivery and tissue engineering." *Biomaterials* 29, no. 13 (2008): 1989-2006. https://doi.org/10.1016/j.biomaterials.2008.01.011

[28] Kim, Hong Nam, Alex Jiao, Nathaniel S. Hwang, Min Sung Kim, Deok-Ho Kim, and Kahp-Yang Suh. "Nanotopography-guided tissue engineering and regenerative medicine." *Advanced drug delivery reviews* 65, no. 4 (2013): 536-558. https://doi.org/10.1016/j.addr.2012.07.014

[29] Mahjour, Seyed Babak, Farshid Sefat, Yevgeniy Polunin, Lichen Wang, and Hongjun Wang. "Improved cell infiltration of electrospun nanofiber mats for layered tissue constructs." *Journal of Biomedical Materials Research Part A* 104, no. 6 (2016): 1479-1488. https://doi.org/10.1002/jbm.a.35676

[30] Morel, Alexandre, Anne Géraldine Guex, Fabian Itel, Sebastian Domaschke, Alexander E. Ehret, Stephen J. Ferguson, Giuseppino Fortunato, and René M. Rossi. "Tailoring the multiscale architecture of electrospun membranes to promote 3D cellular infiltration." *Materials Science and Engineering: C* 130 (2021): 112427. https://doi.org/10.1016/j.msec.2021.112427

[31] Barbosa, M. A., I. C. Gonçalves, P. M. D. Moreno, R. M. Gonçalves, S. G. Santos, A. P. Pêgo, and I. F. Amaral. "2.13 Chitosan." (2017): 279-305. https://doi.org/10.1016/b978-0-12-803581-8.10246-2